

Dual Electron Uptake by Simultaneous Iron and Ligand Reduction in an N-Heterocyclic Carbene Substituted [FeFe] Hydrogenase Model Compound

Jesse W. Tye, Jonghyuk Lee, Hsiao-Wan Wang, Rosario Mejia-Rodriguez, Joseph H. Reibenspies, Michael B. Hall,* and Marcetta Y. Darensbourg*

Department of Chemistry, Texas A&M University, College Station, Texas 77843-3255

Received March 17, 2005

An N-heterocyclic carbene containing [FeFe] H_2 ase model complex, whose X-ray structure displays an apical carbene, shows an unexpected two-electron reduction to be involved in its electrocatalytic dihydrogen production. Density functional calculations show, in addition to a one-electron Fe–Fe reduction, that the aryl-substituted N-heterocyclic carbene can accept a second electron more readily than the Fe–Fe manifold. The juxtaposition of these two one-electron reductions resembles the [FeFe] H_2 ase active site with an FeFe di-iron unit joined to the electroactive 4Fe4S cluster.

The hydrogenase enzymes catalyze the reversible reduction of protons to dihydrogen: $2H^+ + 2e^- \leftrightarrow H_2$,¹ utilizing dinuclear active sites comprised of sulfur-bridged [NiFe] or [FeFe] assemblies. In a nonbiological setting, proton reduction and H_2 oxidation are normally most readily accomplished at a platinum electrode. Almost immediately after their discovery, the prospect of replacing such expensive catalysts by these base metal-containing enzymes was recognized. In fact, when absorbed onto a graphite electrode, the [NiFe] hydrogenase enzyme from *Allochrodatum vinosum* has been shown to function as a heterogeneous catalyst for H_2 oxidation.² Although the [NiFe] enzymes are generally more thermally and O_2 stable,¹ the [FeFe] enzyme active site has proven to be more amenable to small-molecule-model studies because of its resemblance to well-known organometallic complexes of the type $(\mu-SR)_2[Fe^I(CO)_2L]_2$.³ We and others have found that these complexes function as solution electrocatalysts for H_2 production.^{4–7}

As compared to the biocatalysts, the model complexes synthesized to date require strong acids and/or much more negative reduction potentials to produce H_2 . The difference could lie in the substitution pattern and donor strength of

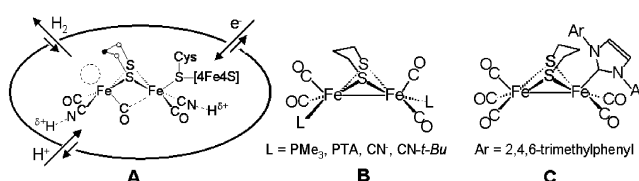


Figure 1. Comparison of the enzyme active site (A), symmetrically substituted model complexes (B), and an asymmetrically substituted model complex (C).

the non-CO ligands, as shown in Figure 1. Density functional theory (DFT) calculations suggest that an asymmetrically substituted complex that has one end locked into position by a sterically encumbered ligand with excellent donating ability might have special features conducive to H_2 electrocatalysis.⁸ We have thus prepared the N-heterocyclic carbene containing model compound, $(\mu-S(CH_2)_3S)[Fe(CO)_3][Fe(CO)_2IMes]$, **1-IMes** [IMes = 1,3-bis(2,4,6-trimethylphenyl)imidazol-2-ylidene; Figure 1C]. The X-ray-derived molecular structure is given in Figure 2.

Herein we report that the asymmetric **1-IMes** complex in the presence of a weak acid (HOAc) shows electrocatalytic activity. This complex is particularly exciting as an electrocatalyst because it appears that the conjunction of Fe and IMes ligand valence orbitals permits the uptake of two electrons at the same potential.

In the absence of a proton source, **1-IMes** in CH_3CN undergoes one irreversible reduction at -1.70 V (vs NHE) and two irreversible oxidations at 0.51 and 1.12 V. The

* To whom correspondence should be addressed. E-mail: mbhall@tamu.edu (M.B.H.), marcetta@mail.chem.tamu.edu (M.Y.D.).

(1) Cammack, R.; Frey, M.; Robson, R. *Hydrogen as a Fuel: Learning from Nature*; Taylor & Francis: London, 2001.
(2) Lamle, S. E.; Vincent, K. A.; Halliwell, L. M.; Albracht, S. P. J.; Armstrong, F. A. *Dalton Trans.* **2003**, 4152.

(3) (a) Lyon, E. J.; Georgakaki, I. P.; Reibenspies, J. H.; Darensbourg, M. Y. *Angew. Chem., Int. Ed.* **1999**, *38*, 3178. (b) Le Cloirec, A.; Davies, S. C.; Evans, D. J.; Hughes, D. L.; Pickett, C. J.; Best, S. P.; Borg, S. *Chem. Commun.* **1999**, 2285. (c) Schmidt, M.; Contakes, S. M.; Rauchfuss, T. B. *J. Am. Chem. Soc.* **1999**, *121*, 9736.
(4) Chong, D.; Georgakaki, I. P.; Mejia-Rodriguez, R.; Sanabria-Chinchilla, J.; Soriaga, M. P.; Darensbourg, M. Y. *Dalton Trans.* **2003**, 4158.
(5) Gloaguen, F.; Lawrence, J. D.; Rauchfuss, T. B.; Bénard, M.; Rohmer, M.-M. *Inorg. Chem.* **2002**, *41*, 6573.
(6) Mejia-Rodriguez, R.; Chong, D.; Reibenspies, J. H.; Soriaga, M. P.; Darensbourg, M. Y. *J. Am. Chem. Soc.* **2004**, *126*, 12004.
(7) Borg, S. J.; Behrsing, T.; Best, S. P.; Razavet, M.; Liu, X.; Pickett, C. J. *J. Am. Chem. Soc.* **2004**, *126*, 16988.
(8) Bruschi, M.; Fantucci, P.; De Gioia, L. *Inorg. Chem.* **2004**, *43*, 3733.

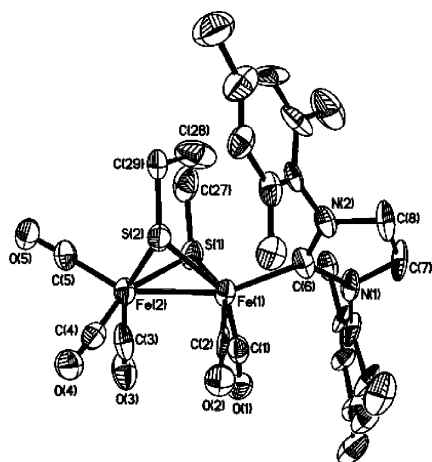


Figure 2. Molecular structure of **1-IMes** (TEP at 50% probability). Hydrogen atoms are omitted for clarity.

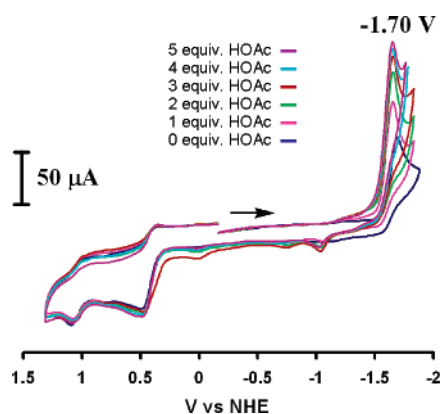


Figure 3. CVs of **1-IMes** (2.0 mM) with HOAc (0–10 mM) in a CH_3CN solution (0.1 M $n\text{-Bu}_4\text{NBF}_4$) with a glassy carbon electrode at a scan rate of 200 mV s^{-1} .

observed irreversibility of the reduction peak at -1.70 V is most likely not due to CO loss. Even at low temperature ($-15 \text{ }^\circ\text{C}$) and fast scan rates (20 V s^{-1}), CO-saturated solutions of **1-IMes** show no sign of reversibility. The **1-IMes** complex was investigated as an electrocatalyst for dihydrogen production from a weak acid. The addition of 1–5 equiv of HOAc to a 2.0 mM CH_3CN solution of **1-IMes** (Figure 3) shows an enhancement of the peak current for the reduction wave at -1.70 V , while having very little effect on the remainder of the cyclic voltammogram (CV). This result is consistent with electrocatalytic H_2 production.^{4,6}

Controlled-potential coulometry for **1-IMes** demonstrated the event at -1.70 V to be a two-electron-reduction process in the absence of added acid. The two-electron assignment for **1-IMes** was confirmed by the following control experiment: when the total charge (Q) passed during the bulk electrolysis at an applied potential of -1.80 V approached a calculated value of ~ 1.25 electrons per **1-IMes** molecule, the bulk electrolysis was stopped and a CV was obtained on this solution. A noticeable reduction wave remained at -1.70 V , indicating incomplete reduction of the bulk solution (Figure 4). Interestingly, this is in contrast to one-electron reduction previously observed for a series of $\text{Fe}^{\text{I}}\text{Fe}^{\text{I}}$ dithiolate complexes.^{4,5} For direct comparison, the controlled-potential experiment was performed for the analogous monophosphine

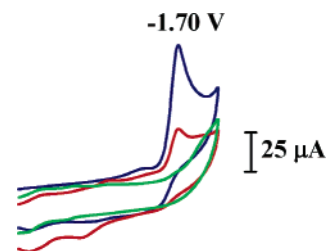


Figure 4. CVs of **1-IMes** (1.0 mM) in a CH_3CN solution (0.1 M $n\text{-Bu}_4\text{NBF}_4$) before bulk electrolysis (blue), after the passage of a total charge equivalent to 1.25 electrons (red), and after the passage of a total charge equivalent to 2.10 electrons (green).

complex, **1-PTA** (PTA = 1,3,5-triaza-7-phosphaadamantane), under identical conditions, and clearly showed a one-electron-reduction process, as previously reported.⁵

DFT has proven itself a valuable tool for addressing the molecular details of electrochemical problems.⁹ To better understand the nature of **1-IMes** and the reduced species $[\mathbf{1-IMes}]^-$ and $[\mathbf{1-IMes}]^{2-}$, DFT calculations were undertaken on these species, assuming compositional integrity. The optimized structure of **1-IMes** overlays well with the molecular structure derived from X-ray crystallography. The HOMO and LUMO of **1-IMes** are predominantly Fe–Fe bonding and Fe–Fe antibonding, respectively. Because the first added electron occupies an Fe–Fe antibonding orbital, the main structural change upon geometry optimization of $[\mathbf{1-IMes}]^-$ is elongation of the Fe–Fe bond from 2.52 to 2.80 Å. From the unpaired Fe spin densities of 0.22 and 0.99 of the $\text{Fe}(\text{CO})_3$ and $\text{Fe}(\text{CO})_2(\text{IMes})$ units, respectively, the $[\mathbf{1-IMes}]^-$ species is assigned as an $\text{Fe}^0\text{Fe}^{\text{I}}(\text{IMes}^0)$ species. That is, the added electron is localized on the $\text{Fe}(\text{CO})_3$ moiety, benefiting from the delocalization of three CO ligands.

The addition of a second electron to **1-IMes** can conceivably lead to either a second Fe–Fe-based reduction or an IMes ligand based reduction. If the second reduction is Fe-based, then a singlet state should result from the two thiolate-bridged low-spin pseudotrigonal-pyramidal Fe^0 centers. If the second reduction is IMes ligand based, then a triplet state should result from the unpaired electrons in the IMes ligand and the Fe–Fe manifold. Single-point energy calculations on species formed upon the addition of a second electron, $[\mathbf{1-IMes}]^{2-}$, constrained at the $[\mathbf{1-IMes}]^-$ geometry, show that the lowest energy triplet state is $5.3 \text{ kcal mol}^{-1}$ more stable than the lowest energy singlet state, column II of Figure 5. Geometry optimization of the singlet and triplet structures of $[\mathbf{1-IMes}]^{2-}$ reverses this energy difference and finds the triplet structure $7.0 \text{ kcal mol}^{-1}$ higher in energy than the singlet structure, column III of Figure 5. Geometry optimization of the singlet state of $[\mathbf{1-IMes}]^{2-}$, which has a formal Fe–Fe bond order of 0, leads to a nonbonding Fe–Fe distance of 3.39 Å. The singlet structure of $[\mathbf{1-IMes}]^{2-}$ is therefore assigned as an $\text{Fe}^0\text{Fe}^0(\text{IMes}^0)$ species.

Geometry optimization of the triplet state of $[\mathbf{1-IMes}]^{2-}$, which has a formal Fe–Fe bond order of $1/2$, leads to an

(9) (a) Patterson, E. V.; Cramer, C. J.; Truhlar, D. G. *J. Am. Chem. Soc.* **2001**, *123*, 2025. (b) Baik, M.-H.; Ziegler, T.; Schauer, C. K. *J. Am. Chem. Soc.* **2000**, *122*, 9143.

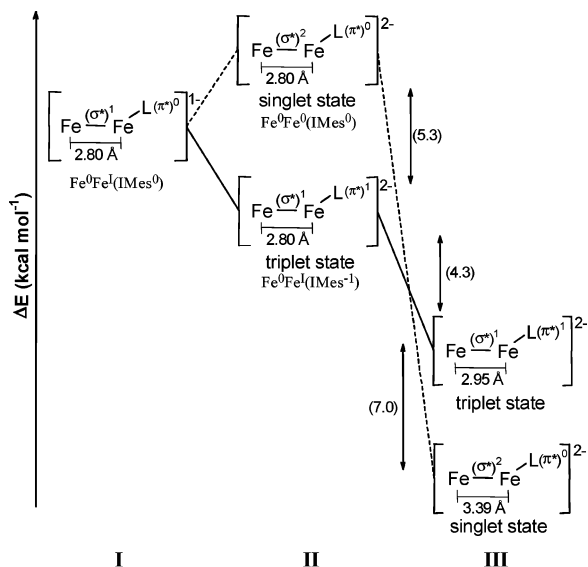


Figure 5. Energies and Fe–Fe distances for the geometry-optimized $[1\text{-IMes}]^-$ (I), singlet and triplet states for $[1\text{-IMes}]^{2-}$ at the $[1\text{-IMes}]^-$ geometry (II), and fully optimized structures of $[1\text{-IMes}]^{2-}$ (III).

Fe–Fe distance of 2.95 Å. It is noteworthy that the Fe–Fe distance in the triplet structure of $[1\text{-IMes}]^{2-}$ lies much closer to that of $[1\text{-IMes}]^-$ than that of singlet $[1\text{-IMes}]^{2-}$. Mulliken spin analysis of the optimized triplet structure computes unpaired spin densities of 0.07 and 1.23 on the irons of the $\text{Fe}(\text{CO})_3$ and $\text{Fe}(\text{CO})_2(\text{IMes})$ units, respectively. A total spin density of 0.91 is on the IMes ligand: 8.0% on the carbenoid carbon and 79.7% on the carbon atoms of the aryl rings. A total spin density of -0.20 is spread over the five CO ligands. The triplet state of $[1\text{-IMes}]^{2-}$ is therefore assigned as an $\text{Fe}^0\text{Fe}^1(\text{IMes}^{-1})$ species.

In other words, $[1\text{-IMes}]^-$ immediately produced at the electrode surface upon reduction of **1-IMes**, represented as I in Figure 5, may then accept a second electron into the redox-active NHC ligand.¹⁰ Alternatively, $[1\text{-IMes}]^-$ may accept a second electron into the Fe–Fe antibonding orbital, yielding a singlet state. The former possibility is more likely because electron transfer is a fast process and the lower energy triplet state of $[1\text{-IMes}]^{2-}$ results in only a small overall structural change from $[1\text{-IMes}]^-$, whereas production of the singlet state results in a major structural change. In support of this hypothesis, the $\text{Fe}^1\text{Fe}^0 + e^- \rightarrow \text{Fe}^0\text{Fe}^0$ reduction is not observed for the monophosphine complex.⁶

The extended π system present in the IMes ligand is apparently a requirement for this type of carbene-based reduction to occur. Computations on a simplified model of $[1\text{-IMes}]^{2-}$, in which the 2,4,6-trimethylphenyl rings have been replaced by hydrogen atoms, predict the lowest energy

triplet state to arise from the coupling of two $S = 1/2$ Fe^0 centers and not from one-electron reductions of the Fe–Fe manifold and the NHC ligand.

During the review of this Communication, Capon et al. published a synthetic and electrochemical study of an apically substituted N-heterocyclic carbene complex of the form $(\mu\text{-S}(\text{CH}_2)_3\text{S})[\text{Fe}(\text{CO})_3][\text{Fe}(\text{CO})_2(\text{L}_{\text{Me}})]$ [$\text{L}_{\text{Me}} = 1,3\text{-bis}(\text{methyl})\text{-imidazol-2-ylidene}$].¹¹ Their complex undergoes *one-electron reduction* at -1.66 V vs NHE in CH_3CN . Their finding of a single one-electron reduction for the bis(methyl)carbene is consistent with our computation on the small model of the IMes ligand.

From previous electrochemical results on the monophosphine complex, **1-PTA**, we proposed an ECCE mechanism for H_2 production by **1-PTA** in the presence of the weak acid, HOAc.⁵ For **1-IMes**, however, it is more likely that a two-electron reduction (one electron at the Fe–Fe center and one electron on the IMes ligand) precedes protonation at iron to yield an $[\text{HFeFe}]^-$ moiety. A second protonation and internal electron transfer from the reduced IMes ligand to the iron center result in the release of dihydrogen and regeneration of the Fe^1Fe^1 starting material. Overall, the electrochemical process is described as an EECC mechanism. A similar mechanism was proposed for H_2 production by cofacial bisorganometallic diruthenium and diosmium porphyrins.¹²

In summary, the use of the IMes ligand permits the uptake of two electrons at the same reduction potential, resulting in a change in mechanism from that observed for the closely related monophosphine and monocarbene complexes. DFT calculations suggest that this difference in mechanism arises from the involvement of the IMes ligand as an electroactive participant. By analogy to the $[\text{FeFe}]_{\text{H}_2\text{ase}}$ site, the electroactive IMes ligand may serve as a model for the electroactive $4\text{Fe}4\text{S}$ cluster.

Acknowledgment. We acknowledge financial support from the National Science Foundation (Grant CHE-0111629 to M.Y.D. and Grant CHE-9800184 to M.B.H.) and the R.A. Welch Foundation (Grant A-0924 to M.Y.D. and Grant A-0648 to M.B.H.). We thank Dr. Daesung Chong for initiating the electrochemical studies of **1-IMes**. We also thank the Supercomputing Facility and the Tensor Beowulf cluster (NSF Grant MRI-0216275) at Texas A&M University for computer time.

Supporting Information Available: X-ray structural data for **1-IMes**, synthetic, electrochemical, and computational details, and CIF data. This material is available free of charge via the Internet at <http://pubs.acs.org>.

IC050402D

(10) Gorodetsky, B.; Ramnial, T.; Branda, N. R.; Clyburne, J. A. C. *Chem. Commun.* **2004**, 1972.

(11) Capon, J.-F.; El Hassnaoui, S.; Gloaguen, F.; Schollhammer, P.; Talarmin J. *Organometallics* **2005**, *24*, 2020.

(12) Collman, J. P.; Ha, Y.; Wagenknecht, P. S.; Lopez, M. A.; Guilard, R. J. *Am. Chem. Soc.* **1993**, *115*, 9080.